Healing of Nanocracks by Disclinations

G. Q. Xu* and M. J. Demkowicz

Department of Materials Science and Engineering, Massachusetts Institute of Technology (MIT), Cambridge, Massachusetts 02139, USA

(Received 24 May 2013; published 2 October 2013)

We present a new mechanism—discovered using molecular dynamics simulations—that leads to complete healing of nanocracks. This mechanism relies on the generation of crystal defects known as disclinations by migrating grain boundaries. Crack healing by disclinations does not require any compressive loads applied normal to the crack faces and even occurs under monotonic tensile loading. By closing small cracks and suppressing the propagation of others, this mechanism may provide a novel way of mitigating internal damage that influences ductility in nanocrystalline metals.

DOI: 10.1103/PhysRevLett.111.145501 PACS numbers: 61.72.Lk, 61.46.Hk, 61.72.Mm, 62.20.mt

Nanocrystalline (NC) metals with grain sizes below 100 nm have high strength [1], but low ductility: they often fail due to necking [2,3] or fracture [4–6] before any significant uniform plastic deformation occurs. While much work has been done to prevent necking in NC materials [7–9], less is known concerning how to suppress fracture. In this work, we describe a mechanism whereby the generation and motion of crystal defects known as disclinations [10] leads to complete healing of nanocracks.

The key process in the crack healing mechanism we wish to describe is stress-driven grain boundary migration (SDGBM). In SDGBM, a shear stress applied parallel to a grain boundary leads to diffusionless migration of the boundary in the direction perpendicular to its plane. Numerous modeling [11] and experimental [12,13] studies have recently been performed on SDGBM. To understand how SDGBM influences fracture, we use molecular dynamics (MD) to simulate loading of a model microstructure in nickel (Ni): a bicrystal, shown in Fig. 1(a), with a pre-existing nanocrack. The nanocrack is stable when no external stress is applied.

The model is loaded in shear by applying tractions along the surfaces normal to the z direction [14]. Because of the symmetry of the stress tensor, both GB1 and GB2, shown in Fig. 1(a), are under shear stress. The orientations of grain 1 and grain 2 are chosen such that GB1 is a symmetric tilt grain boundary (GB). GB1 consists of an array of parallel edge dislocations [see inset of Fig. 1(a)] and migrates easily due to their collective motion under an applied load [15]. Reversing the loading direction reverses the migration direction of GB1. GB2 does not undergo shear-coupled migration and its shear resistance is sufficiently high so that it does not shear during the simulation.

We found that the migration of GB1 causes the nanocrack to open or close, depending on the direction of migration. This is surprising since the system is loaded under pure shear: there is never any net tensile or compressive external load applied to it. When GB1 moves away from the crack, the crack surfaces initially undergo a reversible crack opening displacement, as if the system were experiencing net tensile load (see Supplemental Material movie 1, [14]). At an average engineering shear strain of 3.5%, Shockley partial dislocations nucleate at the crack tip and glide into grain 2, as illustrated in Fig. 1(b). Additional dislocations are emitted as GB1 continues to migrate and the crack extends into grain 2.

However, when GB1 moves toward the crack, the crack surfaces progressively close as illustrated in Fig. 1(c) and the Supplemental movie 2 [14], even though no net compressive stress is applied. As GB1 continues to migrate, the crack faces eventually come into contact and rapidly bond along the entire length of the crack. The nanocrack is thereby fully healed, leaving behind several edge

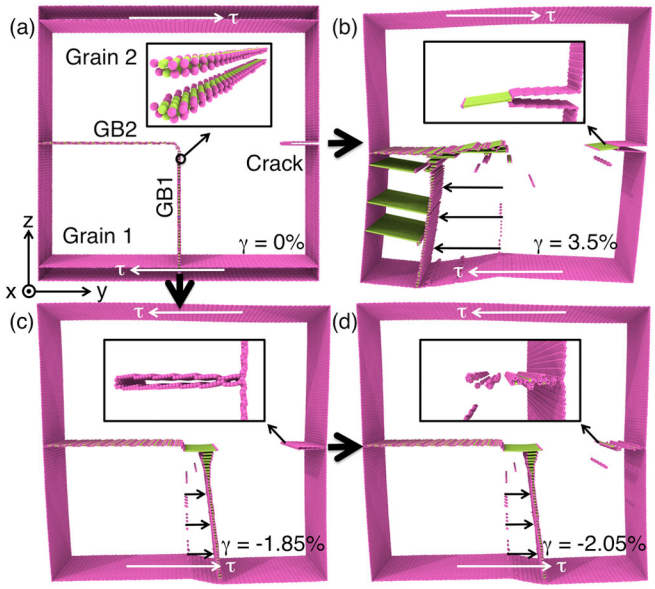

FIG. 1 (color online). (a) Ni bicrystal model with a nanocrack. The inset shows dislocations in GB1. The crack opens (b) when GB1 moves away from it, but closes (c) and eventually heals completely (d) when GB1 moves towards it. All perfect crystal atoms have been suppressed for clarity.

dislocations with Burgers vectors pointing in the surface normal direction of the original crack [see Fig. 1(d)]. Their presence in the vicinity of the healed crack is topologically necessary because the crack itself was formed by the removal of a ~1 nm-thick layer of atoms.

Crack opening and closing in the presence of SDGBM may be interpreted using the mechanics of crystal defects known as disclinations [10]. Figure 2 illustrates how "positive" and "negative" wedge disclinations are created. For a positive one [Fig. 2(a)], a wedge of material of angle ω is removed. The surfaces thereby created are then forced together and welded shut. For a negative wedge disclination [Fig. 2(b)], a cut is made and the surfaces thereby created are forced open to an angle ω. A wedge of material is welded in to close the gap.

Figures 2(c)–2(e) illustrate how wedge disclination dipoles may be used to describe the effect of GB migration on internal stress fields [16,17]. If surfaces MN and MKL are not connected, then GB1 migration produces the shear offset shown in Fig. 2(c). To reconnect surfaces MN and MKL, a positive wedge disclination is added at point M in Fig. 2(d) to close the gap $\angle NMK$ and a negative wedge disclination is added at point K in Fig. 2(e) to prevent overlap in region ΔLKN. The σ_{zz} (tensile) stress field calculated from the simulations in Fig. 1 at 1.5% applied shear strain and shown in Fig. 2(f) and 2(g) gives clear evidence of discrete, well separated, clearly identifiable disclinations at the predicted locations. The stress field of each disclination translates with the disclination as it moves during SDGBM.

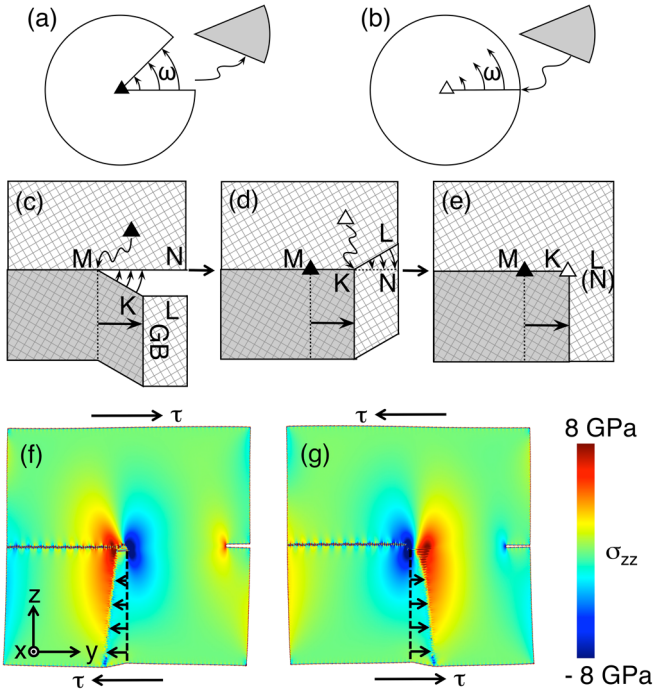

FIG. 2 (color online). (a) Positive (filled triangle) and (b) negative (open triangle) wedge disclinations. (c) If surfaces MN and MKL are not connected, then GB migration produces the shear offset shown. (d) A positive wedge disclination is added at M to close the gap $\angle NMK$. (e) A negative wedge disclination is added at K to prevent overlap in ΔLKN. (f) σ_{zz} field when GB1 migrates away from the crack and (g) toward the crack. Positive and negative disclinations coincide with the compressive (blue) and tensile (red) stress concentrations, respectively.

The presence of disclinations is also confirmed directly from the atomistic configurations by conducting a Burgers circuit analysis [18]. The disclination strength, which is calculated as the path-independent rotational closure failure along a circuit around the disclination core, is equal to the misorientation angle of GB1 (see Supplemental Material Fig. 1, [14]). This agrees with the value predicted using the GB migration model in Fig. 2. The Burgers circuit analysis also justifies the use of discrete disclinations, instead of modeling internal stresses created during SDGBM with arrays of hypothetical dislocations.

The internal stresses generated by migrating GBs in an infinite solid may be computed analytically by superimposing the stress fields of positive and negative wedge disclinations, which have been known for over a century [19]. In a finite solid, a disclination dipole will additionally induce tractions on the free surfaces. Therefore, image stresses will arise to satisfy traction-free boundary conditions [20]. It is these image stresses that are responsible for the crack healing mechanism described here. To substantiate this claim, we used the finite element method (FEM) to assess the effect of surface image stresses on the disclination-induced deformation of the model shown in Fig. 1. The directions and magnitudes of relative crack surface displacements calculated from the image stresses alone are in excellent quantitative agreement with atomistic simulations as are the stress fields calculated by FEM (see Supplemental Material Figs. 3 and 4, [14]).

Although free surface image stresses are not present at internal intergranular cracks, disclinations formed during SDGBM may still cause the cracks to open or close. Wedge disclinations may attenuate or amplify crack tip stress intensities of internal cracks [21], leading to additional, mixed-mode crack surface displacements. This effect, known as shielding or antishielding, may be expressed as a change in the stress intensity at the crack tip, ΔK. For a disclination dipole lying on the crack plane ahead of a semi-infinite crack,

$$\Delta K_I = \frac{\sqrt{2}}{2}\frac{\mu\omega}{2\pi(1-\nu)}\left(\sqrt{d_+}-\sqrt{d_-}\right), \qquad (1)$$

where μ is the shear modulus, ν is Poisson's ratio, ω the disclination strength, and $d_{+(-)}$ the distance from the crack tip to the positive (negative) wedge disclination.

Equation (1) predicts that larger GB migration distances lead to larger ΔK_I magnitudes and therefore a stronger influence on the crack. Subscript "I" indicates that the stress intensity generated by the disclinations is equivalent

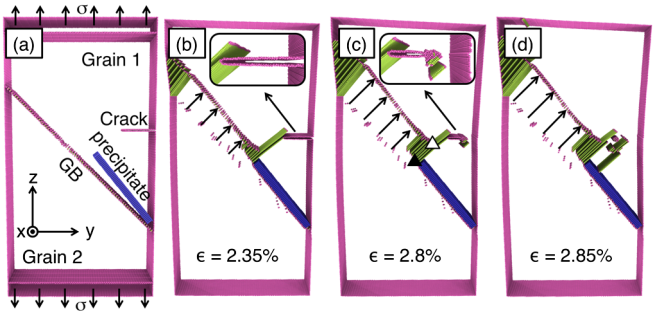

FIG. 3 (color online). (a) Initial configuration and loading conditions. (b) Crack opens slightly due to applied tensile load; the GB begins to migrate towards the crack; part of the GB is blocked by the rigid precipitate. (c) Crack begins to heal as the part of the GB not blocked by the precipitate migrates further; white and black triangles indicate negative and positive disclinations, respectively [see Fig. 2(a)]. (d) Complete crack healing. All perfect crystal atoms have been suppressed for clarity.

to mode I (tensile or compressive) loading [22] and gives rise to crack opening when $d_+ > d_-$ and closing when $d_+ < d_-$. Healing of periodic (semi-infinite) as well as finite-length internal intergranular cracks through this mechanism is demonstrated by MD simulations in the Supplemental Material, movies 3, 4, and 5 (see also movie captions in the Supplemental Material) [14].

A firm understanding of the disclination-based mechanism of crack healing enables us to design microstructures that heal cracks even under monotonic external tensile loading, which would normally cause crack opening and advance. In Fig. 3(a), we show a bicrystal containing a nanocrack and a symmetric tilt GB designed to migrate towards the crack under an applied tensile load. Since the uniform migration of a GB alone would not change the internal stress distribution in a bicrystal and therefore would not influence crack face displacements, we placed an impenetrable precipitate ahead of the advancing GB to block the motion of part of the GB. The precipitate, shown in blue in Fig. 3(a), is created by requiring all the atoms in it to displace as a rigid body.

Tensile loading is applied on the surfaces normal to the z direction. The crack surfaces initially open under the applied load and the GB migrates as expected (see Supplemental Material movie 6, [14]). With further loading, part of the GB impinges upon the impenetrable precipitate while the remainder continues to move, as shown in Fig. 3(b). With continued loading, the crack surfaces cease opening and eventually begin to close. Figure 3(c) shows the moment when the crack faces touch and the crack begins to heal while in Fig. 3(d) the crack has healed completely. Thus, we have successfully designed a microstructure where GB migration is used to achieve a counterintuitive result: complete crack healing under monotonic applied tensile loading.

The stress field inside the bicrystal corresponds to that of the disclination dipole shown in Fig. 3(c). This dipole would not have formed had there been nothing to impede the migration of part of the GB. As the unimpeded section of the GB continues to migrate, it leaves behind a positive wedge disclination near the precipitate while the negative wedge disclination, shown as an open triangle in Fig. 3(c), approaches the crack. The resulting disclination dipole induces closing displacements on the crack surface, which compete with the opening displacements arising from the external load. At a critical GB migration distance, the net displacement of the crack surface switches from opening to closing and the crack eventually heals despite the continuing tensile loading.

The effect of SDGBM on crack healing and advance in Ni is not symmetrical: less migration is required to heal cracks than to advance them. Figure 4 plots crack length as a function of GB migration distance for the simulation shown in Fig. 1. The crack begins to close once GB1 moves towards it by 7.2 nm. However, dislocation emission does not occur until GB1 has migrated 27.7 nm away from the crack. The simulation illustrated in Fig. 1 was repeated with the misorientation of GB1 reversed such that its effect on the crack is reversed: migration away from the crack closes it and migration towards the crack opens it. As shown in Fig. 4, the amount of migration required to heal the crack in this case is again smaller than that required to advance it.

This asymmetry has potentially far-reaching consequences: it suggests that in materials where GBs are equally likely to move towards cracks or away from them, SDGBM-induced crack healing will occur more frequently than SDGBM-induced crack advance. Thus, SDGBM may inhibit fracture by closing small cracks and impeding the formation or propagation of others. It is especially relevant to NC materials because GB-related mechanisms such as GB sliding and SDGBM often play

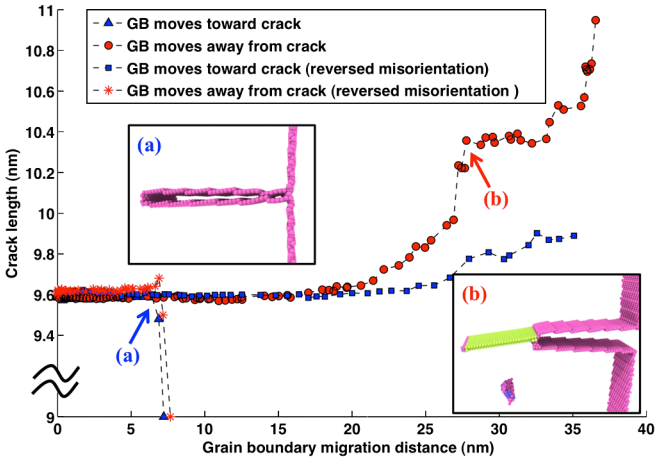

FIG. 4 (color online). The relationship between crack length and GB1 migration distance.

a larger role in their deformation than does conventional dislocation plasticity [23,24]. This proposition is consistent with studies that reported enhanced ductility in NC materials where SDGBM occurred [25–27]. The frequency of disclination-induced crack healing in real microstructures is not currently known. However, studies of fracture in nanopillars and nanowires suggest that direct experimental investigations of such phenomena are becoming possible [28,29].

Disclination formation is not restricted to migrating GBs of the type modeled here. A wide range of GBs is known to undergo stress-driven migration [30] and each of them may give rise to disclinations, albeit possibly of mixed (as opposed to pure wedge) character, depending on the character of the migrating GB. Complete crack healing, however, does depend on the state of the crack surfaces, which will bond together fully only if free of organic debris and passivating scales.

Because disclinations are topological defects, they are stable against local atomic rearrangements. Long-range mass transport due to diffusional flow may relax the high stresses associated with disclinations, but only becomes appreciable at temperatures greater than half the melting temperature and at low strain rates characteristic of creep [31]. Thus, the mechanism described here applies to a broad range of temperatures and strain rates of technological interest.

Other processes besides disclination-induced crack healing influence ductility in NC metals, for instance nanovoid formation or small-scale flow localization [32,33]. Disclination-induced crack healing, however, provides a novel way of mitigating internal damage. It may be used in conjunction with the methods of grain boundary engineering [34] to create microstructures tailored to maximize crack healing, yielding new classes of fracture-resistant NC materials with both high strength and ductility.

This work was funded by the BP-MIT Materials and Corrosion Center. We are grateful to S. Gradečak, D. M. Parks, and W. Curtin for insightful discussions.

*To whom all correspondence should be addressed.
gqxu@mit.edu

[1] J. Schiøtz and K. W. Jacobsen, Science **301**, 1357 (2003).
[2] Y. H. Zhao, T. T. Zhu, and E. J. Lavernia, Adv. Eng. Mater. **12**, 769 (2010).
[3] E. Ma, Nat. Mater. **2**, 7 (2003).
[4] K. M. Youssef, R. O. Scattergood, K. L. Murth, J. A. Horton, and C. C. Koch, Appl. Phys. Lett. **87**, 091904 (2005).
[5] H. Q. Li and F. Ebrahimi, Appl. Phys. Lett. **84**, 4307 (2004).
[6] Y. M. Wang, K. Wang, D. Pan, K. Lu, K. J. Hemker, and E. Ma, Scr. Mater. **48**, 1581 (2003).
[7] Y. M. Wang, M. W. Chen, F. H. Zhou, and E. Ma, Nature (London) **419**, 912 (2002).
[8] X. L. Wu, Y. T. Zhu, Y. G. Wei, and Q. Wei, Phys. Rev. Lett. **103**, 205504 (2009).
[9] L. Lu, X. Chen, H. Huang, and K. Lu, Science **323**, 607 (2009).
[10] A. E. Romanov, Eur. J. Mech. A. Solids **22**, 727 (2003).
[11] Z. T. Trautt, A. Adland, A. Karma, and Y. Mishin, Acta Mater. **60**, 6528 (2012).
[12] T. J. Rupert, D. S. Gianola, Y. Gan, and K. J. Hemker, Science **326**, 1686 (2009).
[13] B. Beausir and C. Fressengeas, Int. J. Solids Struct. **50**, 137 (2013).
[14] See Supplemental Material at http://link.aps.org/supplemental/10.1103/PhysRevLett.111.145501 for the detailed methods and the animations of the crack healing simulations.
[15] C. H. Li, E. H. Edwards, J. Washbum, and E. R. Parker, Acta Metall. **1**, 223 (1953).
[16] I. A. Ovid'ko, A. G. Sheinerman, and E. C. Aifantis, Acta Mater. **56**, 2718 (2008).
[17] S. V. Bobylev, N. F. Morozov, and I. A. Ovid'ko, Phys. Rev. Lett. **105**, 055504 (2010).
[18] E. Kroner and K. H. Anthony, Annu. Rev. Mater. Sci. **5**, 43 (1975).
[19] V. Volterra, Annales scientifiques de l'ENS **24**, 401 (1907).
[20] J. P. Hirth and J. Lothe, *Theory of Dislocations* (Wiley, New York, 1982), 2nd ed.
[21] Q. H. Fang, Y. W. Liu, C. P. Jiang, and B. Li, Eng. Fract. Mech. **73**, 1235 (2006).
[22] K. B. Broberg, *Cracks and Fracture* (Academic Press, London, 1999), p. 46.
[23] V. Yamakov, D. Wolf, S. R. Phillpot, A. K. Mukherjee, and H. Gleiter, Nat. Mater. **3**, 43 (2004).
[24] K. W. Jacobsen and J. Schiøtz, Nat. Mater. **1**, 15 (2002).
[25] T. H. Fang, W. L. Li, N. R. Tao, and K. Lu, Science **331**, 1587 (2011).
[26] D. S. Gianola, S. Van Petegem, M. Legros, S. Brandstetter, H. Van Swygenhoven, and K. J. Hemker, Acta Mater. **54**, 2253 (2006).
[27] L. Lu, L. B. Wang, B. Z. Ding, and K. Lu, J. Mater. Res. **15**, 270 (2000).
[28] F. Östlund, P. R. Howie, R. Ghisleni, S. Korte, K. Leifer, W. J. Clegg, and J. Michler, Philos. Mag. **91**, 1190 (2011).
[29] C. Peng, Y. Zhan, and J. Lou, Small **8**, 1889 (2012).
[30] J. W. Cahn and J. E. Taylor, Acta Mater. **52**, 4887 (2004).
[31] H. J. Frost and M. F. Ashby, *Deformation-Mechanism Maps:The Plasticity and Creep of Metals and Ceramics* (Pergamon Press, Oxford, 1982).
[32] D. Farkas, M. Willemann, and B. Hyde, Phys. Rev. Lett. **94**, 165502 (2005).
[33] Y. Yang, B. Imasogie, G. J. Fan, P. K. Liaw, and W. O. Soboyejo, Metall. Mater. Trans. A **39**, 1145 (2008).
[34] D. T. Fullwood, S. R. Niezgoda, B. L. Adams, and S. R. Kalidindi, Prog. Mater. Sci. **55**, 477 (2010).